Evolutionary and Deterministic Methods for Design,
Optimization and Control with Applications to Industrial and Societal Problems
EUROGEN 2005
R. Schilling, W.Haase, J. Periaux, H. Baier, G. Bugeda (Eds)

MINIMIZATION OF THE WAVE DRAG OF A FLEET OF SUPERSONIC AIRCRAFTS

Yuichiro Goto[⋆], **Shinkyu Jeong**[*], **Shigeru Obayashi**[†] **and Yasuaki Kohama**[‡]

[⋆] Ultimate Flow Environment Laboratory,
Institute of Fluid Science, Tohoku University
2-1-1 Katahira, Aoba-ku, Sendai, Japan
e-mail: gotoh@ltwt.ifs.tohoku.ac.jp,
web page: http://www.ifs.tohoku.ac.jp/Kohama-lab/~gotoh

[*] Integrated Fluid Informatics Laboratory,
Institute of Fluid Science, Tohoku University
2-1-1 Katahira, Aoba-ku, Sendai, Japan
e-mail: jeong@edge.ifs.tohoku.ac.jp, web page: http://www.ifs.tohoku.ac.jp/edge

[†] Integrated Fluid Informatics Laboratory,
Institute of Fluid Science, Tohoku University
2-1-1 Katahira, Aoba-ku, Sendai, Japan
e-mail: obayashi@ifs.tohoku.ac.jp, web page: http://www.ifs.tohoku.ac.jp/edge

[‡] Ultimate Flow Environment Laboratory,
Institute of Fluid Science, Tohoku University
2-1-1 Katahira, Aoba-ku, Sendai, Japan
e-mail: kohama@ifs.tohoku.ac.jp, web page: http://www.ifs.tohoku.ac.jp/Kohama-lab/

Key words: Supersonic Transport, Wave Drag, Sonic Boom, Formation Flying, Kriging, Optimization

Abstract. *In this study, design of a formation of three supersonic aircrafts is carried out. The objective is to minimize the total wave drag of the formation, and to maximize the separation of the aircrafts for safety. Kriging has been used to search for better formations in a limited amount of computation. Results show a improvement in the objectives with each iteration step, and good agreement was obtained between past studies and trends of the generated solutions.*

1 INTRODUCTION

In the past 50 years, many attempts have been made to realize commercially practical civil supersonic transports. The two major problems that have prevented supersonic commercial transportation are wave drag and sonic boom. Wave drag, which is the dominating component of drag at supersonic speeds, leads to a deterioration in cruise efficiency. And sonic booms have a problem of public acceptance.

Many attempts have been made to minimize the wave drag and the sonic boom via aircraft shape optimization. However, results have shown a strong trade-off between wave drag and sonic boom, making it impossible to minimize wave drag and sonic boom simultaneously.

As a different approach to overcoming these problems, the use of formation flying in supersonic speeds for the simultaneous reduction of wave drag and sonic boom, was proposed.[1]

When an aircraft flies through the air at supersonic speeds, they leave momentum in the air behind them. This is the cause of wave drag. Wave drag of the following aircraft is reduced by collecting this momentum as pressure gradient.

The reduction of sonic boom of the fleet will be achieved by virtual elongation. It is a well known fact that the pressure signature of the sonic boom is dependent on the overall length and the area distribution of the aircraft. This area distribution is defined by a sweep of a plane inclined downward at the Mach angle. If the aircrafts are placed in a way such that the area distribution of the aircraft are clustered together, this will result in an elogated pressure wave, consequently reducing the boom intensity.

In the previous study,[1] sensitivity analysis has been carried out on two aircraft formations. In this case, the flow pattern was simple and intuitive, and the formations in the analysis were generated from intuition on the flow field.

In the current study, the objective is to gain insight on the drag reduction of three aircraft formations. The flow patterns are expected to be more complicated and less intuitive in three aircraft formations, making it impractical to generate the formations from intuition. Therefore, in this study, design will be carried out on three aircraft formations in a more objective manner.

For objective design, optimization using Kriging is carried out. Kriging was chosen taking into account the fact that expensive Euler computations are used for the flow analysis. This method makes it possible to optimize the formation to a certain level in a limited amount of computation.

2 PROBLEM DEFINITION

In this study, the objectives are chosen to be the maximization of the total L/D of the formation and the maximization of minimum of the separations between the aircrafts. The first objective is considered for improving the cruise efficiency, and the second objective is considered to maximize the safety and the tolerance of the position keeping.

The design variables are the coordinates of the two following aircrafts.

In the coordinate system used in this analysis, x is in the freestream direction, y is out towards the right wing tip, and z is upward. The origin of the coordinate system is located at the half chord position along the centerline of the leading aircraft. The coordinates are normalized by the root chord of the aircraft.

The previous study has shown that shock interaction is the most important physics in the drag reduction.[1] Therefore, a skewed cylindrical coordinate expression, which effectively extracted the physics, is used as the design variables that define the relative position of the aircrafts.

In this definition, the position of the following aircraft is expressed using three parameters r, θ and x_μ. The conversion from the cylindrical coordinate expression to the Cartesian expression is given by,

$$\begin{aligned} x &= x_{i_{Cone}} + x_\mu + r/\tan\mu \\ y &= y_{i_{Cone}} + r\ \sin\theta \\ z &= z_{i_{Cone}} + -r\ \cos\theta \end{aligned}$$

First of all, r is a parameter to express how far away along the Mach cone, the following aircraft is located from of the leading aircraft. However, the value of r is not defined as the distance along the Mach cone, but as the distance between the longitudinal axes of the leading and following aircrafts. Next, θ is the azimuthal position in the yz plane, defined in proper right hand coordinate system, and $\theta = 0°$ is defined to be pointing downwards in the $-z$ direction. And finally, x_μ expresses the streamwise position of the following aircraft with respect to the Mach cone extending downstream from the center of the leading aircraft. Although there are small discrepancies due to nonlinearity, x_μ can be regarded as a parameter that indicates how the following wing interacts with the shock and expansion waves.[1]

Figure 1 is a diagram showing the relation between the coordinate expressions. In this figure, the conventional coordinate system is drawn in black dashed lines, the Mach cone is drawn in orange lines, and the definition of the skewed cylindrical coordinate system is drawn in green lines.

The leading aircraft, *Aircraft 0*, is defined as the origin of the coordinate system. Next, the coordinates of the first following aircraft, *Aircraft 1*, is defined by the three parameters given above, with the origin of coordinate definition placed at *Aircraft 0*. Finally, the coordinates of the second following aircraft, *Aircraft 2*, is given by the three parameters above, and an integer variable defining on which aircraft the origin of the coordinate definition is placed. In general, this integer variable takes an integer value from the range $[0, i-1]$ for *Aircraft i*. This coordinate definition make it possible to effectively cover the coordinate space where we expect shock interaction, but, at the same time, exclude regions where we expect no shock interaction.

The number of design variables was 7. The design variables and their upper and lower bounds are given in Table 1. Here, the subscripts on the variables denote to which aircraft the variable belongs.

The constraints imposed on the positions of the aircrafts were that the aircrafts must stay inside the outer boundary of the computational mesh, and that the aircrafts must be a certain distance away from each other, for successful mesh generation. The mesh outer boundary was a conical shape with the vertex at $(-3.5, 0, 0)$, and the base is a circle, located at $(5.0, 0, 0)$, with a radius of 8.5. As for the distance, an ellipsoid that is able to enclose the aircraft with a small margin is selected, and distance is defined using this ellipsoid.

Finally, the problem can be given in the following form.

$$
\begin{array}{rlcl}
\textbf{maximize} & \sum_i L_i / \sum_i D_i & & \\
\textbf{maximize} & \min\limits_{i,\,j,\,i\,\neq\,j} \; d_{i,j} & & \\
 & & & \\
\textbf{subject to} & \min\limits_{i,\,j,\,i\,\neq\,j} \; x^0_{\mu\,i} & > & \text{-2.5} \\
 & \max\limits_{i} \; x_i & < & 4.0 \\
 & \min\limits_{i,\,j,\,i\,\neq\,j} \; d'_{i,j} & > & 2.0
\end{array}
$$

Where,

$$
\begin{aligned}
(r^0_i,\, \theta^0_i,\, x^0_{\mu\,i}) &= \boldsymbol{F}_0^{\mathbf{-1}}\,(\,\boldsymbol{F}_{iCone}\,(r_i,\, \theta_i,\, x_{\mu\,i})\,) \\
d(i,j) &= ((x_i - x_j)/1.0)^2 + ((y_i - y_j)/1.2)^2 + ((z_i - z_j)/0.1)^2
\end{aligned}
$$

Here, $\boldsymbol{F}_{iCone}$ is the coordinate conversion function, and r^0, θ^0, $x^0_{mu\,i}$ are the cylindrical coordinate parameters converted to $iCone = 0$.

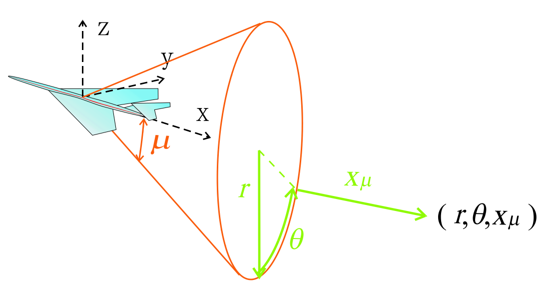

Figure 1: Definition of the new coordinate parameters

Variable	Type	Bounds
r_1	real	[0, 3.0]
$theta_1$	real	[-4.0, 4.0]
$x_{\mu\,1}$	real	[-2.0, 2.0]
r_2	real	[0, 3.0]
$theta_2$	real	[-4.0, 4.0]
$x_{\mu\,2}$	real	[-2.0, 2.0]
i_{Cone_2}	integer	[0, 1]

Table 1: Design variables and their bounds

3 METHOD

3.1 Optimization

In this study, optimization is carried out using a combination of Latin Hypercube sampling, Kriging and multi-objective genetic algorithm. The steps of the optimization is given next.

1. Generate initial solutions.

2. Evaluate objective and constraint function values.

3. Generate a response surface.

4. Evaluate the estimated objective values and the uncertainties to choose new solutions to add to the response surface.

5. If satisfied with the accuracy, exit. Else, goto 2.

First of all, initial solutions are generated using Latin Hypercube sampling. Here, it was made sure that the solutions satisfy the constraints. The objective and constraint functions are evaluated using an Euler flow solver and simple geometry. Details on the flow solver will be mentioned in section 3.2.

Next, response surface is generated from the solutions using Kriging. Kriging is a statistics based response surface method that is able to estimate both the function values and the their uncertainties. In this method, the unknown function of interest is expressed as

$$y(\boldsymbol{x}) = \mu + Z(\boldsymbol{x})$$

where μ is a constant global model for the unknown function, and $Z(\boldsymbol{x})$ is the random deviation from that model. To model this function, a linear predictor,

$$\hat{y} = c^T(\boldsymbol{x})\,\boldsymbol{y}$$

is identified by minimizing the mean squared error subject to an unbiasedness constraint, using Lagrange Multipliers and optimality condition.[2] Here, $\boldsymbol{y}$ is the vector of the evaluated function values. Then, Kriging model used in this study is obtained in the following form.

$$\hat{y} = \hat{\mu} + \boldsymbol{r}^T \boldsymbol{R}^{-1}(\boldsymbol{y} - \mathbf{1}\hat{\mu})$$

and,

$$\hat{\mu} = \frac{\mathbf{1}^T \boldsymbol{R}^{-1} \boldsymbol{y}}{\mathbf{1}^T \boldsymbol{R}^{-1} \mathbf{1}}$$

The mean squared error is given by

$$s^2(\boldsymbol{x}) = \hat{\sigma}^2 \left[1 - \boldsymbol{r}^T \boldsymbol{R}^{-1} \boldsymbol{r} + \frac{\left(1 - \mathbf{1}^T \boldsymbol{R}^{-1} \mathbf{1}\right)^2}{\mathbf{1}^T \boldsymbol{R}^{-1} \mathbf{1}} \right]$$

Where,

$$\hat{\sigma}^2 = \frac{(\boldsymbol{y} - \mathbf{1}\hat{\mu})^T \boldsymbol{R}^{-1} (\boldsymbol{y} - \mathbf{1}\hat{\mu})}{n}$$

$\boldsymbol{R}$ is the matrix of correlation between the evaluated Zs, and $\boldsymbol{r}$ is the correlation vector between the Z to be estimated and the evaluated Zs. Since the correlation of Z is strongly dependent on the distance between the two solutions, a weighted distance and a Gaussian random function will be used as the correlation.

$$d(\boldsymbol{x_i}, \boldsymbol{x_j}) = (\boldsymbol{x}_i - \boldsymbol{x}_j)^T \boldsymbol{\Theta} (\boldsymbol{x}_i - \boldsymbol{x}_j)$$

where, $\boldsymbol{\Theta}$ is a matrix with the weights as the diagonal elements. Using this weighted distance, the correlation will be defined as,

$$Corr\left(Z(\boldsymbol{x}_i), Z(\boldsymbol{x}_k)\right)) = \exp\left(-d(\boldsymbol{x}_i, \boldsymbol{x}_j)\right)$$

$\boldsymbol{r}$ and $\boldsymbol{R}$ can finally be written as,

$$\boldsymbol{r}_j(\boldsymbol{x}) = \exp\left(-d(\boldsymbol{x}, \boldsymbol{x}_j)\right)$$

$$\boldsymbol{R}_{i,j} = \exp\left(-d(\boldsymbol{x_i}, \boldsymbol{x}_j)\right)$$

The log-likelihood function of the sampled solutions can be written as,

$$-\frac{n}{2} ln(2\pi) - \frac{n}{2} ln(\hat{\sigma}^2) - \frac{1}{2} ln\left(|\boldsymbol{R}|\right) - \frac{1}{2\hat{\sigma}^2} (\boldsymbol{y} - \mathbf{1}\hat{\mu})^T \boldsymbol{R}^{-1} (\boldsymbol{y} - \mathbf{1}\hat{\mu})$$

Therefore, the problem will be an unconstrained optimization problem of minimizing,

$$-\frac{n}{2} ln(\hat{\sigma}^2) - \frac{1}{2} ln\left(|\boldsymbol{R}|\right)$$

with respect to the weighting parameter matrix $\boldsymbol{\Theta}$. In the current problem definition, design variable *iCone* is an integer variable. Therefore, the Kriging surface is generated separately for each value *iCone* takes, for each objective function.

To evaluate the estimated objectives and the uncertainties simultaneously, a figure of merit called Expected Improvement is used.[3] In case of a maximization problem, Expected Improvement is defined,

$$EI(\boldsymbol{x}) = E\left(max(Z - y_{\max}, 0)\right)$$

where, $y_{\max}$ the maximum objective value of the sampled solutions. Solving for the expected value, the Expected Improvement results in,

$$EI(\boldsymbol{x}) = (\hat{y} - f_{\max})\,\Phi\left(\frac{\hat{y} - f_{\max}}{s}\right) + s\,\phi\left(\frac{\hat{y} - f_{\max}}{s}\right)$$

where, ϕ and Φ are the probability density function and the cumulative distribution function of the Gaussian distribution. The process of maximizing the Expected Improvement is carried out via genetic algorithm for use in Multi-Objective problems[4].

And finally, to evaluate the convergence of the Kriging model, cross-validation is carried out by excluding and estimating one sampled solution, and comparing their values.

3.2 Flow Computation

Since the objective of this study is to investigate the effectiveness of supersonic formation flying, the subject of the analysis is kept simple. For this reason, the model used for this study is a simple elliptical planform wing with a biconvex airfoil.

Although simplification of the configuration is convenient, the drag characteristic of the simplified model must be similar to that of a practical supersonic transport. The aspect ratio and thickness are determined to satisfy this condition.[1] This resulted in an elliptic wing with the following dimensions.

Aspect Ratio	:	1.5
Normalized Span	:	$1.5\pi/4$
Thickness Ratio	:	0.04502
Wing Area	:	0.9253

A three view diagram of this configuration is given in Fig.2.

The freestream Mach number used in this analysis is $M = 1.5$. This Mach number was chosen considering recent trends in the cruise Mach number of recent supersonic transports concepts. The angle of attack of the wings are maintained at $\alpha = 3.25°$. This angle of attack is chosen so that the C_L of the leading wing which is flying in undisturbed freestream equals 0.146.

The computational mesh used in this analysis is an unstructured full three-dimensional mesh with 1.05 million grid points, and 21,000 grid points on each wing. The cross-section of this mesh at $y = 0$ is given in Fig.3. A full three dimensional mesh is used to allow for asymmetric formations.

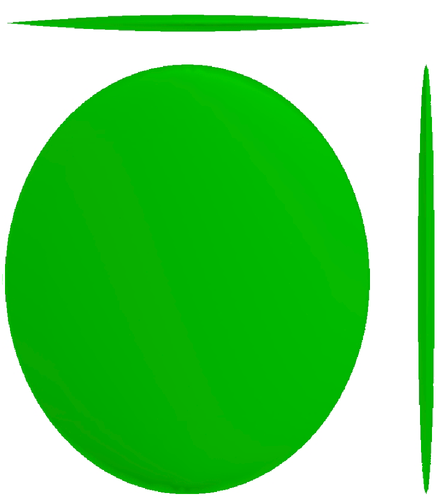

Figure 2: Three view diagram of simplified model

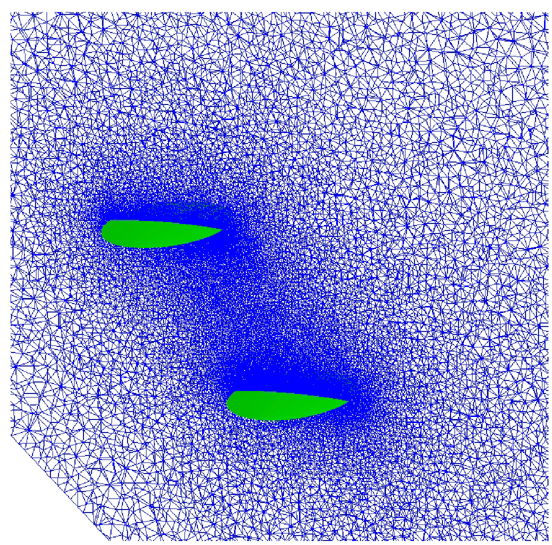

Figure 3: Symmetry plane of computational mesh

Euler simulations are carried out using *TAS-flow*, an unstructured Euler/Navier-Stokes solver, and the computational mesh was generated using *EdgeEditor* and *TU TetraGrid*, which are CFD tools developed at Tohoku University.

TAS-flow is an unstructured Euler/Navier-Stokes solver using a finite-volume cell-vertex scheme, HLLEW Riemann solver for flux computations,[5] and LU-SGS implicit scheme for time integration.[6] *EdgeEditor* is an unstructured surface mesh generation software. It takes CAD data as an input,[7] and generates a surface mesh using an advancing front triangulation method.[8] *TU TetraGrid* is an unstructured volume mesh generation software using the Delaunay triangulation algorithm.[9]

4 RESULTS AND DISCUSSIONS

4.1 Flow Field

To obtain an idea on the flow field, flow computations are carried out on two aircraft formations. Details are given in the previous paper,[1] but two cases will be presented here.

First of all, when $(r,\, \theta,\, x_\mu) = (1.23,\, \pi,\, 0.70)$, the following aircraft achieved the best L/D. The C_p contours on the $y = 0$ is shown in Fig.4. The aerodynamic coefficients of the leading and following aircrafts are, $C_L = 0.145$, $C_D = 0.0183$, $L/D = 7.90$ and $C_L = 0.142$, $C_D = 0.0137$, $L/D = 10.4$, respectively, and the total L/D was 8.97. In this case, the leading edge of the following aircraft is exposed to the expansion wave from the leading aircraft, reducing the wave drag.

On the other hand, the following aircraft achieved the worst L/D when $(r,\, \theta,\, x_\mu) = (1.34,\, 0.0,\, 0.00)$. The C_p contours on the $y = 0$ is shown in Fig.5. The aerodynamic

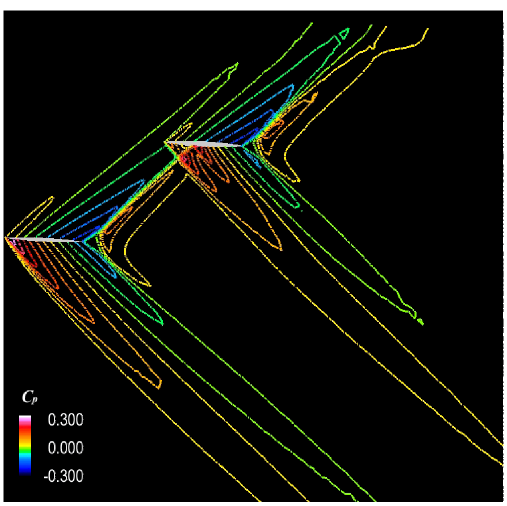

Figure 4: C_p contour of $y = 0$, $(r,\, \theta,\, x_\mu) = (1.23,\, \pi,\, 0.70)$

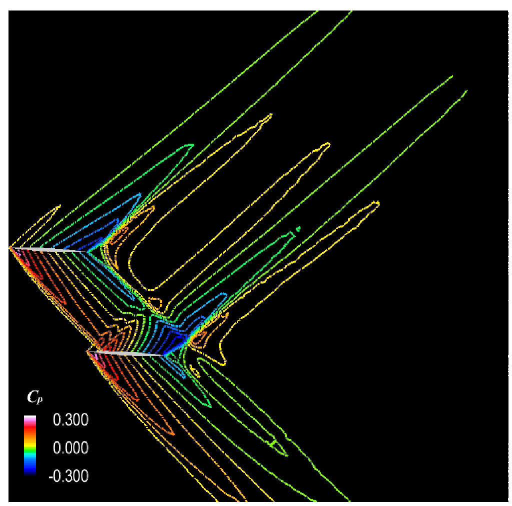

Figure 5: C_p contour of $y = 0$, $(r,\, \theta,\, x_\mu) = (1.34,\, 0.0,\, 0.00)$

coefficients of the leading and following aircrafts are, $C_L = 0.145$, $C_D = 0.0184$, $L/D = 7.89$ and $C_L = 0.071$, $C_D = 0.0153$, $L/D = 4.66$, respectively, and the total L/D was 6.41. In this case, the shock wave extending from the leading edge is impinging on the upper surface of the following aircraft near the leading edge, spoiling the lift and increasing the drag.

The results of the sensitivity analysis of the two aircraft formations indicate that x_μ is the parameter that determines the shock interaction pattern of the following aircraft, and it is the parameter with dominating effect on the L/D of the following aircraft.

4.2 Optimization

Optimization has been carried out on three aircraft formations using the system introduced in Section 3.

Solutions generated by this optimization system is shown in Fig.6 and 7, for $iCone = 0$, $iCone = 1$ respectively. About 20 solutions were generated by Latin Hypercube sampling, and about 15 points are added by 2 or 3 Kriging phases. Solutions generated by Latin Hypercube Sampling are shown in blue symbols, those generated by Kriging in green, yellow and red, in the order that they were generated. Here, the ellipse indicate the region of 90% confidence for each stage of optimization.

Looking at the movement of the ellipse as the iteration proceeds, the solutions are being generated in the direction that the Pareto-optimal solutions are expected to be. When $iCone = 0$, the confidence ellipse for the solutions generated in the second Kriging stage indicates a worse region compared to the confidence ellipse of the first stage of Kriging. This is due to the fact that there was one "unlucky guess" in the solutions generated from the second Kriging stage, and the confidence ellipse is dragged towards that solution.

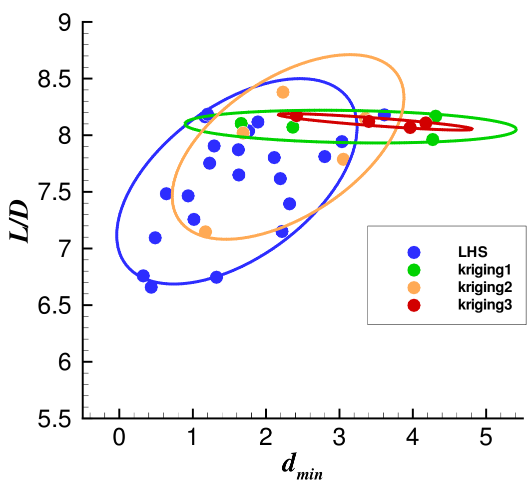

Figure 6: Solutions generated by optimization for $iCone = 0$

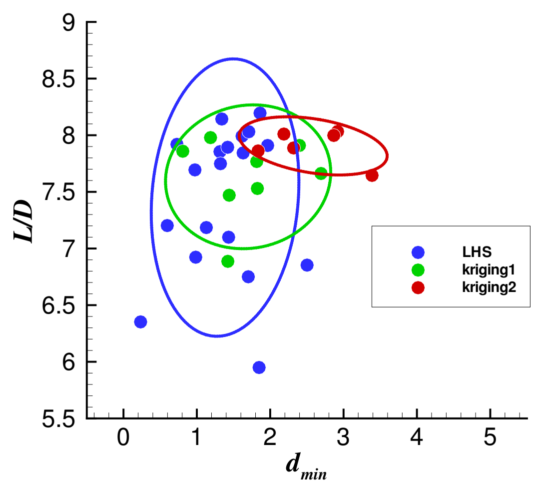

Figure 7: Solutions generated by optimization for $iCone = 1$

So far, among all of the solutions generated, three non-dominated solutions have been obtained. The objective function values for the three non-dominated solutions were, $(L/D, d_{min}) = (8.38, 2.23)$, $(8.18, 3.61)$ and $(8.17, 4.31)$.

First, strongly non-dominated solution $(L/D, d_{min}) = (8.38, 2.23)$ is investigated. This solution obtained the maximum L/D among all of the solutions. The coordinates, and the aerodynamic coefficients of the aircrafts were,

	x	y	z	C_L	C_D	L/D
Aircraft 0	0.0	0.0	0.0	0.1453	0.0184	7.90
Aircraft 1	1.93	-0.69	-1.01	0.1490	0.0177	8.43
Aircraft 2	3.74	-0.22	-2.23	0.1593	0.0181	8.82

$$d_{0,1} = 2.29 \qquad d_{1,2} = 2.23 \qquad d_{2,0} = 4.36$$

When the coordinates for the following aircrafts are converted to the skewed cylindrical expression using the relation given in Section 2, x_{mu} for *Aircraft 1* and *2* are 0.56 and 1.23. This corresponds to a position where *Aircraft 1* is in a position where $x_\mu = 0.56$ with respect to the *Aircraft 0*, and *Aircraft 2* is in a position such that $x_\mu = 0.67$ with respect to *Aircraft 1*. Insight from the previous study indicates that flying in a position such that $x_\mu \approx 0.5$ is very effective in improving the cruise efficiency of the following aircraft, therefore agrees very well with the current results.

However, the L/D of each of the aircrafts do not achieve the value that the previous study achieves. This can either be due to the trade-off between the maximization of L_1/D_1 and maximization of L_2/D_2 or due to the fact that solution is not yet optimal.

On the other hand, the coordinates and the aerodynamic coefficients for strongly non-dominated solution for minimum separation distance were,

	x	y	z	C_L	C_D	L/D
Aircraft 0	0.0	0.0	0.0	0.1452	0.0184	7.89
Aircraft 1	4.00	-1.84	1.65	0.1476	0.0178	8.29
Aircraft 2	3.70	2.21	-0.04	0.1556	0.0187	8.32

$$d_{0,1} = 4.70 \qquad d_{1,2} = 4.40 \qquad d_{2,0} = 4.31$$

In this case, the constraint on the maximum value of x is active. This bounds the objective d_{min}, and further improvement in this objective cannot be expected.

But, when the coordinates are converted to the skewed cylindrical expression, $x_\mu \approx 1.23$ for both cases. Since there are no other constraints active, improvements in the cruise performance can be expected with a similar value of minimum separation distance by adjusting the position of the aircrafts such that $x_\mu \approx 0.5$. Also, the previous study indicates that effect of shock interaction is reduced as displacements in the y direction is introduced. Therefore, improvements in L/D can be expected by changing values of θ_1 and θ_2.

As mentioned before, the solutions obtained from optimization agreed very well with the insight gained in the previous paper. However, this also indicates that the three aircraft formations obtained so far has only been a combination of two aircraft formations, meaning that aircrafts are only affected by one other aircraft. It is intuitively easy to imagine that best performance will be obtained when the last aircraft is receiving beneficial effect from both the two leading aircrafts. Therefore, further evaluation of solutions will be carried out to search for such formations and evaluate their performance.

By using the skewed cylindrical coordinate expression as the design variables, it was possible to generate solutions only in the region where there is shock interaction between the aircrafts. However, in this coordinate definition, formations obtained for $iCone = 0$ may also be obtained for $iCone = 1$. This indicates that there is a redundant degree of freedom in this coordinate definition, and results in an unnecessary expansion of the design space, increasing the necessary number of evaluation. Therefore, in future study, solutions should be converted from $iCone = 0$ to $iCone = 1$ and vice versa, and be used in generating the Kriging surface to cover the the design space more effectively in the limited amount of computation time.

5 CONCLUSIONS

In this study, Kriging has been applied to the design of formations of three supersonic aircrafts for low drag supersonic flights and maximum separation between the aircrafts. Optimization results have shown improvements towards Pareto-optimal solutions.

Solutions obtained during the optimization agree well with insight gained in past studies. On the other hand, the solutions obtained so far has been too intuitive in the sense that all solutions are only an extension of the two aircraft formations. Therefore, optimization will be continued to find innovative solutions which have a synergetic effect on the performance.

A skewed cylindrical coordinate expression was used for the design variables to cover only the regions where the pressure waves interact with the aircrafts. This expression effectively searched the design space, but optimization exploited the fact that there is a redundant degree of freedom in the problem definition. In future study, this redundancy must be eliminated for a more effective search and a more accurate Kriging response surface.

As for the design space exploration, the current number of solutions was not enough to gain insight on the relation with the constraints and the design variables. Plans for future study include, further addition of solutions using Kriging and the exploration of the design space to clarify the relation between the objectives and the design variables.

REFERENCES

[1] Y. Goto, S. Obayashi, and Y. Kohama, Drag Characteristics of a Low-Drag Low-Boom Supersonic Formation Flying Concept, *AIAA Paper*, 2005-4604, 2005.

[2] J. Sacks, W. J. Welch, T. J. Mitchell, and H. P. Wynn, Design and Analysis of Computer Experiments, *Statistical Science*, **4** , No. 4, 409–435, 1989.

[3] D. R. Jones, M. Schonlau, and W. J. Welch, Efficient Global Optimization of Expensive Black-Box Functions, *Journal of Global Optimization*, **13** , 455–492, 1998.

[4] S. Jeong, K. Yamamoto, and S. Obayashi, Kriging-Based Probablistic Method for Constrained Multi-Objective Optimization Problem, *AIAA Paper*, 2004-6437, 2004.

[5] S. Obayashi and G. P. Guruswamy, Convergence Acceleration of an Aeroelastic Navier-Stokes Solver, *AIAA Journal*, **33** , No. 6, 1134–1141, 1994.

[6] D. Sharov and K. Nakahashi, Reordering of Hybrid Unstructured Grids for Lower-Upper Symmetric Gauss-Seidel Computations, *AIAA Journal*, **36** , No. 3, 484–486, 1998.

[7] Y. Ito and K. Nakahashi, Surface Triangulation for Polygonal Models Based on CAD Data, *International Journal for Numerical Methods in Fluids*, **39**, Issue 1, 75–96, 2002.

[8] Y. Ito and K. Nakahashi, Direct Surface Triangulation Using Stereolithography Data, *AIAA Journal*, **40** , No. 3, 490–496, 2002.

[9] D. Sharov and K. Nakahashi, A Boundary Recovery Algorithm for Delaunay Tetrahedral Meshing, *Proceedings of the 5^{th} International Conference on Numerical Grid Generation in Computational Field Simulations*, 229–238, 1996.